Bond-orientational order and Frank's constant in two-dimensional colloidal hard spheres

Alice L Thorneywork[1,2], **Joshua L Abbott**[1], **Dirk G A L Aarts**[1], **Peter Keim**[3] **and Roel P A Dullens**[1]

[1] Department of Chemistry, Physical and Theoretical Chemistry Laboratory, University of Oxford, South Parks Road, Oxford, OX1 3QZ, United Kingdom
[2] Cavendish Laboratory, University of Cambridge, Cambridge CB3 0HE, United Kingdom
[3] Department of Physics, University of Konstanz, Konstanz 78464, Germany

E-mail: roel.dullens@chem.ox.ac.uk

CrossMark

Abstract

Recently, the full phase behaviour of 2D colloidal hard spheres was experimentally established, and found to involve a first order liquid to hexatic transition and a continuous hexatic to crystal transition (Thorneywork *et al* 2017 *Phys. Rev. Lett.* **118** 158001). Here, we expand upon this work by considering the behaviour of the bond-orientational correlation time and Frank's constant in the region of these phase transitions. We also consider the excess entropy, as calculated from the radial distribution functions, for a wide range of area fractions covering the liquid, hexatic and crystal phases. In all cases, the behaviour of these quantities further corroborates the previously reported melting scenario of 2D colloidal hard spheres.

(Some figures may appear in colour only in the online journal)

1. Introduction

The spatial dimensionality of a system can have a profound effect upon its physical properties. This may be observed in both structural and dynamic phenomena, with examples including the absence of long-range translational order in a 2D crystal [1] and the differing diffusive behaviour seen in one and two dimensions [2, 3]. Another notable and widely studied example is the melting transition in 2D. Here, unlike melting in 3D [4], it is proposed that an additional 'hexatic' phase exists between the 2D liquid and crystalline phases. This results in melting via two consecutive phase transitions, a scenario described by the KTHNY theory from Kosterlitz, Thouless, Halperin, Nelson and Young [5–8].

More specifically, KTHNY theory links the melting of 2D materials to the unbinding of topological defects. The three key types of defects—dislocation pairs, dislocations and disclinations—all consist of five- or seven-fold coordinated particles, and are illustrated in figure 1. Crystalline states in 2D possess quasi-long-ranged translational order and long-ranged bond-orientational order and the only type of defect consistent with this is a dislocation pair, which is composed of two five-fold and two seven-fold coordinated particles (see figure 1(a)). Clearly shown here is that the presence of a bound dislocation pair in a crystal does not disrupt the translational or bond-orientational order of the crystal. The softening of the shear elasticity of the crystal in the vicinity of the crystal-hexatic transition can be linked to the presence of these dislocation pairs and is described by a recursion relation: as more dislocation pairs appear the crystal becomes increasingly soft, which in turn increases the probability of the creation of new dislocation pairs, which further softens the crystal. At the crystal-hexatic transition, bound dislocation pairs unbind into isolated dislocations as a result of which the shear elasticity disappears [6–8]. A dislocation, consisting of a five-fold and a seven-fold coordinated particle, is shown in figure 1(b), and leads to a loss of translational order but the retention of bond-orientational order. The resulting hexatic phase is therefore
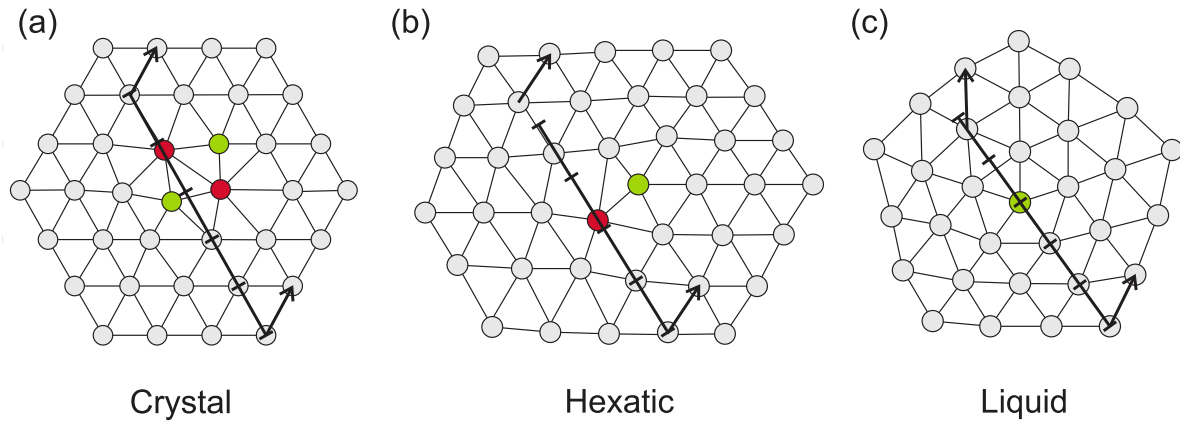
Figure 1. An illustration of the defects seen in the melting of 2D crystals: (a) a dislocation pair; (b) a dislocation; and (c) a 5-fold disclination. Particles coloured red are those with seven nearest neighbours and particles coloured green are those with five nearest neighbours. Arrows indicate the bond-orientation on each side of the defect and lines mark the particle positions expected for systems with translational order.

characterised by short-ranged translational order and quasi-long-ranged six-fold bond-orientational order. The second step of melting to an isotropic fluid is associated with the unbinding of dislocations to form isolated five- and seven-fold disclinations (see figure 1(c)), which disrupt the system with respect to both the translational and bond-orientational order. The resulting liquid phase thus has only short-ranged translational and short-ranged bond-orientational order.

The spatial range of the bond-orientational order is quantified by the bond-orientational correlation function [9, 10]

$$g_6(r) = \mathrm{Re} \left\langle \frac{\psi_{6,i}(r) \cdot \psi_{6,i}^*(0)}{|\psi_{6,i}|^2} \right\rangle, \qquad (1)$$

with the sixfold bond-orientational order parameter, $\psi_{6,i}$, defined as [10]

$$\psi_{6,i}(t) = \frac{1}{n} \sum_{j=1}^{n} \exp(\mathrm{i}6\theta_{ij}(t)). \qquad (2)$$

Here n is the number of nearest neighbours and θ_{ij} is the angle between the vector connecting the central particle, i, with neighbouring particles, j, and a fixed reference axis. At large r $g_6(r)$ attains a constant value in the crystal, but decays algebraically in the hexatic phase, with $g_6(r) \sim r^{-1/4}$ at the transition between the hexatic and liquid [7, 11]. In the liquid, the short-ranged bond-orientational order leads to an exponential decay of $g_6(r)$.

Alternatively, dynamic criteria can be used to distinguish between the liquid, hexatic and crystal states [12], and these are particularly useful for the consideration of experimental systems imaged over a finite distance for a long time. Here, the analogous expression to equation (1) considers the variation in the value of g_6 with time, as [10, 12, 13]

$$g_6(t) = \mathrm{Re} \left\langle \frac{\psi_{6,i}(t) \cdot \psi_{6,i}^*(0)}{|\psi_{6,i}|^2} \right\rangle, \qquad (3)$$

with $\langle ... \rangle$ denoting an average taken over all particles and time origins. For long times, $g_6(t)$ tends towards a constant for the crystal phase whilst in the hexatic phase, $g_6(t)$

decays algebraically as $g_6(t) \sim t^{-\eta_6/2}$, where the exponent $0 < \eta_6 < 1/4$ [7, 10]. Hence, $g_6(t) \sim t^{-1/8}$ at the hexatic-liquid transition [10, 12]. In the liquid phase $g_6(t)$ decays exponentially as $g_6(t) \sim \exp(-t/\tau_6)$ with τ_6 a characteristic bond-orientational correlation time. The exponent η_6 is directly related to the Frank elastic constant F_A as [7, 11]

$$\eta_6 = \frac{18k_\mathrm{B}T}{\pi F_A}, \qquad (4)$$

with k_B Boltzmann's constant and T the temperature. Frank's constant is an effective stiffness of the bond-orientational field, or, in short, an orientational stiffness [11, 14]. Because $\eta_6 = 1/4$ at the liquid-hexatic transition [7, 11], the value of Frank's constant at this transition is $F_A/(k_\mathrm{B}T) = 72/\pi$.

The nature of the 2D melting transition has been extensively studied in computer simulations ever since the introduction of the problem by Alder and Wainwright in 1962 [15]. While it is beyond the scope of this article to provide a comprehensive review of all of these simulations studies, we wish to highlight some more recent advances considering factors known to alter the melting scenario. Firstly, the dependence on interaction potential has been studied for particles with a short-range attraction between them [16] and, over particularly large length scales, for repulsive power-law interactions [17, 18], where the liquid-hexatic transition is found to change from first order to continuous with increasing softness of interaction [18]. For hard core interactions, the particle shape has been observed to effect both the nature of the phases and the order of the transitions [19]. Finally, particularly pertinent to experimental studies, are works considering the effect of pinned particles [20, 21] and out of plane fluctuations [22], which are often found in quasi-2D experiments.

Experimentally, a major body of work considers the phase behaviour of monolayers of super-paramagnetic colloidal particles interacting via a soft potential [9, 11, 12, 23, 24]. For this system, it was established that melting takes place via two consecutive, continuous transitions with an intermediate hexatic phase. Furthermore, the specific heat [25] and elastic constants [11] around the transitions in this system
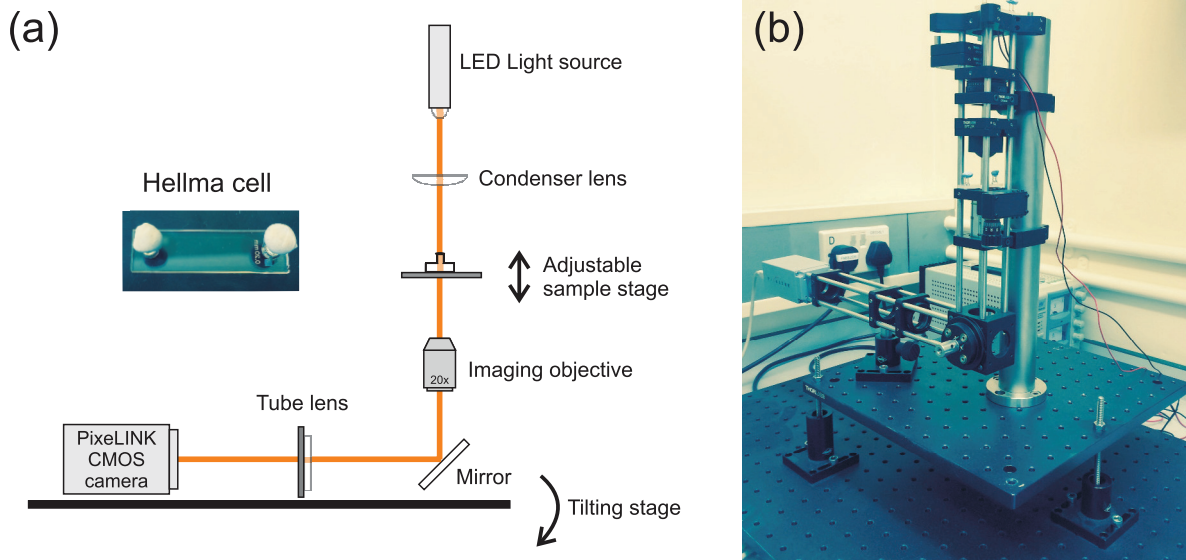
Figure 2. (a) A schematic of the custom-built tilting optical microscopy set-up. Inset: an image of the sample cell used: a Hellma quartz glass cell with internal width of 9 mm, internal length of 20 mm and internal height of 200 μm. (b) A photograph of the tilting microscopy set-up.

have been reported and the effect of random pinning has been addressed [20]. Other experiments have also considered the melting behaviour of charge stabilised systems [26], sticky hard spheres [27, 28] and soft thermosensitive colloidal particles [13, 29].

The simplest interacting many-body system in 2D is a system of thermal hard disks as first studied with computer simulations in 1962 [15]. Inherent to the hard interactions, the phase diagram for hard disks is independent of temperature, and thus only dependent on the area fraction. For hard disks the nature of the melting transition has been the subject of a long and ongoing debate [15, 30–34], but recently large scale computer simulations reported two-step melting via a hexatic phase and a first order liquid-hexatic transition [17, 35]. The two-step melting via a hexatic phase was then also experimentally established [36] by considering a colloidal monolayer in sedimentation-diffusion equilibrium. In particular, in the experiments it was found that melting of the crystal proceeds via a hexatic phase, with a first order liquid-hexatic transition and a coexistence region determined from the equation of state of $\phi \approx 0.68$–0.70. The hexatic phase was observed for $0.70 < \phi < 0.73$ and the continuous hexatic-crystal transition at $\phi \approx 0.73$. In this article, we expand upon these experimental results and consider the behaviour of the bond-orientational correlation time and Frank's constant upon approaching the liquid-hexatic and hexatic-crystal transition, respectively. In addition, we compute the excess entropy from the radial distribution functions for a wide range of area fractions covering the liquid, hexatic and crystal phases.

2. Experimental methods

The experiment has been introduced in [36], so only the essentials will be recapped here. We consider a tilted monolayer of melamine formalydehyde spheres with a hard-sphere

diameter of $\sigma = 2.79$ μm in a water-ethanol mixture. These particles form a monolayer at the base of a glass sample cell (quartz glass Hellma cell, see figure 2(a) inset) and are an excellent hard disk model system [37, 38]. The samples are placed on a custom-built bright-field video microscope, which is then tilted by a small and variable angle, α. In figure 2 we show a schematic (a) and a photograph (b) of the setup. The system is imaged using a 20× objective with images recorded on a PixeLINK CMOS camera at a resolution of 1280 × 1024 pixels. The tilted monolayer is then left to equilibrate for many weeks to reach an in-plane sedimentation-diffusion equilibrium (see figure 1(a) of [36]). The system is imaged at a rate of one frame per sec for 2 h, and standard particle tracking procedures [39] are used to obtain particle coordinates and trajectories.

3. Results and discussion

3.1. Bond-orientational order correlation time

Upon approaching the hexatic phase from the liquid, it has been shown that the bond-orientational correlation length diverges [11]. Consequently, it is also expected that the corresponding bond-orientational correlation time, τ_6, diverges [11, 40, 41]. We determine τ_6 from the bond-orientational correlation functions $g_6(t)$, shown in figure 3(a) for a tilt angle of $\alpha = 0.25°$ [36], via $g_6(t) \sim \exp(-t/\tau_6)$. The bond-orientational correlation time as a function of ϕ upon approaching the hexatic phase from the liquid phase is shown in figure 3(b) for data averaged over all six tilt angles. While at relatively low area fractions τ_6 is about 10 s, it sharply increases upon approaching the first order liquid-hexatic phase transition at $\phi = 0.68$ [36]. This is reminiscent of the critical fluctuations that diverge upon approaching a continuous transition, i.e. critical slowing down. In our case, however, this divergence is
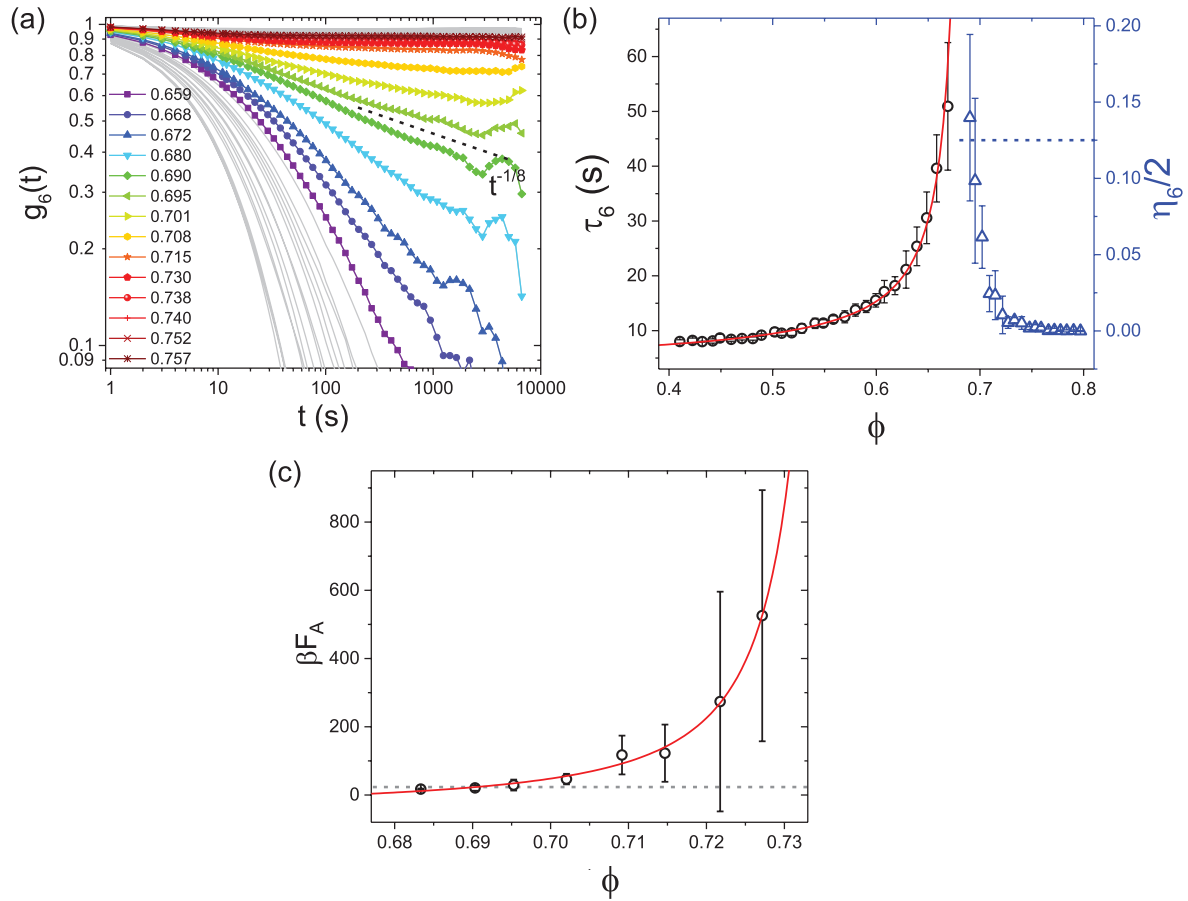
Figure 3. (a) The height-resolved bond-orientational correlation function in time, $g_6(t)$ [36], for the sample at $\alpha = 0.25°$ across the whole range of area fractions. Note that a legend is only provided for the data between $0.65 < \phi < 0.76$. (b) The bond-orientational time τ_6 as a function of the area fraction ϕ. The solid line is a fit according to equation (5). Also shown is the exponent $\eta_6/2$ as a function of the area fraction, whose value of 1/8 indicates the area fraction at which the hexatic phase becomes unstable (see dashed horizontal line). (c) Frank's constant, F_A, as a function of the area fraction ϕ; the symbols are the experimental data and the solid line is a fit to the data according to equation (6). The horizontal straight line corresponds to the value of $72/\pi$, i.e. below which the hexatic phase is unstable. Reprinted figure with permission from [36], Copyright 2017 by the American Physical Society.

preempted by a weakly first order phase transition and hence the bond-orientational correlation time does not diverge. Nevertheless, we can still describe the onset of the divergence of τ_6 for area fractions below the coexistence region using [11, 40, 41]

$$\tau_6 \sim \exp\left[\frac{a}{|1/\phi - 1/\phi_h|^\nu}\right]. \quad (5)$$

Here a is a constant, ϕ_h the area fraction where the system becomes fully hexatic, and the exponent $\nu = 1/2$ [11, 40, 41]. As seen in figure 3(b), the data are very well described by this expression and from the fit we obtain a value for $\phi_h = 0.696$, which is in excellent agreement with the start of the hexatic phase at $\phi = 0.70$ [36]. This is further corroborated by the behaviour of η_6 as a function of ϕ obtained using $g_6(t) \sim t^{-\eta_6/2}$ [10, 36] and also shown in figure 3(b). Here η_6 is close to zero at high area fractions ($\phi > 0.73$), but then starts to increase upon decreasing ϕ and reaches the value of $\eta_6 = 1/4$ at $\phi = 0.70$. In other words, $\phi = 0.70$ is the area fraction where the hexatic phase becomes unstable, consistent with the obtained value of $\phi_h = 0.696$ from fitting equation (5) to our data.

3.2. Frank's constant

Next, we consider the behaviour of Frank's constant, F_A, in the hexatic phase and, in particular, upon approaching the hexatic-crystal transition. Frank's constant is found directly from the exponent η_6 via equation (4) as $\beta F_A = 18/\pi\eta_6$ with $\beta = (k_B T)^{-1}$ and is plotted as a function of ϕ in figure 3(c). At area fractions close to 0.70, i.e. where the hexatic phase starts, βF_A is consistently close to the value of $72/\pi$, i.e. where the hexatic phase is predicted to become unstable. As the area fraction increases, Frank's constant sharply increases and its divergence can be described by [11, 40, 41]

$$\beta F_A \sim \exp\left[\frac{2b}{|1/\phi - 1/\phi_c|^{\bar\nu}}\right]. \quad (6)$$

Here, b is again a constant, ϕ_c the area fraction where the system becomes crystalline and the exponent $\bar\nu = 0.36959$. Our data are well described by equation (6) and from the fit we obtain a value for ϕ_c of 0.733. This is in good agreement with the location of hexatic-crystal transition at ≈ 0.73 [36]—despite the relatively large error bars and the three fitting parameters—and corroborates the continuous nature of this transition.
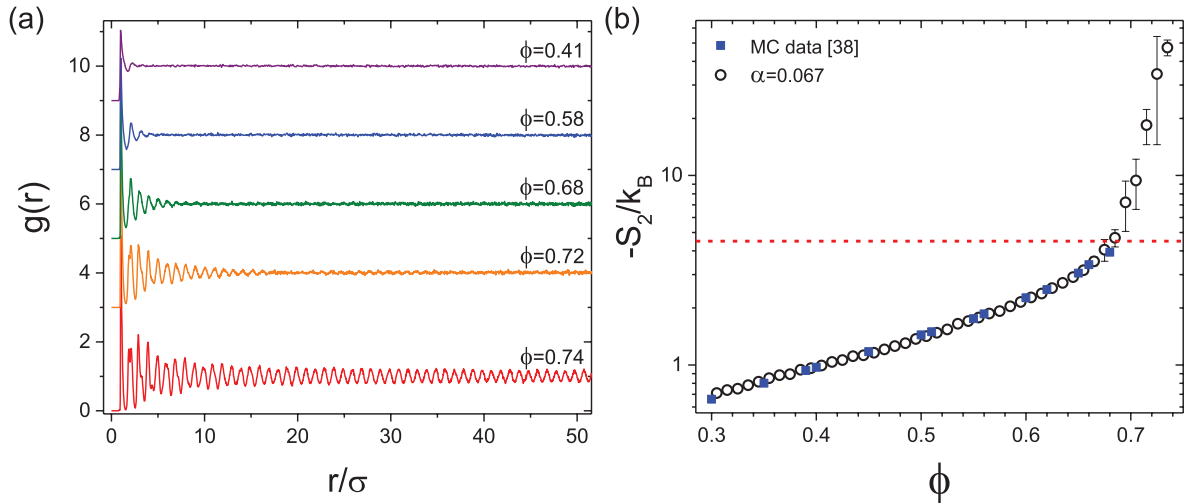
Figure 4. (a) Radial distribution functions, $g(r)$, for area fractions across the liquid, hexatic and crystal phases. Note that they are shifted vertically for clarity. (b) The excess entropy $-S_2/k_B$, calculated from the $g(r)$ via equation (7), as a function of the area fraction ϕ for $\alpha = 0.067°$. The solid line is the melting criterion of $-S_2/k_B = 4.5$ [42] and blue data points show values of $-S_2/k_B$ from MC simulation from [38].

3.3. Excess configurational entropy

Finally, we consider the excess configurational entropy, S_2, as it has been suggested that this can be used as an indicator for freezing in two dimensions [42]. In particular, S_2/k_B, the first term of the excess entropy arising from pair interactions, should attain a universal value of -4.5 at the freezing transition irrespective of the exact nature of the particle interactions [42]. For a 2D system, S_2, is defined by [43]

$$S_2 = -\frac{4k_B\phi}{\sigma^2} \int_0^\infty [g(r)\ln(g(r)) - (g(r) - 1)] \, r\mathrm{d}r, \quad (7)$$

where $g(r)$ is the radial distribution function. To test the S_2 freezing criterion using our data, we first computed the radial distribution functions for different area fractions, which are shown in figure 4(a) for area fractions spanning the liquid, hexatic and crystal phases. At area fractions of 0.41, 0.58 and 0.68 only a small number of peaks are observed, and the structure in $g(r)$ decays rapidly, characteristic of the short ranged translational order in the liquid. For the $g(r)$ in the hexatic phase ($\phi = 0.72$), the range of correlations increases to about 15σ, albeit still being short ranged, while at $\phi = 0.74$ long range correlations in the $g(r)$ are observed, reflecting the quasi-long ranged translational order in the crystal.

Next, we calculated the excess entropy according to equation (7) for a range of area fractions as shown in figure 4(b). At low area fractions, $-S_2/k_B$ increases roughly exponentially with ϕ in agreement with previous reports [38, 44] and is in good agreement with previously reported simulation results for $-S_2/k_B$ in the liquid phase [38]. Around $\phi = 0.65$–0.69, however, there is a marked change in slope, which coincides with the start of the liquid-hexatic coexistence region. In [42] it was reported that at the melting transition $-S_2/k_B$ takes the value of 4.5, which is indicated by the dashed horizontal line in figure 4(b). Our data reach this value at an area fraction of just over $\phi = 0.69$, i.e. just after the change in slope, which approximately corresponds to the start of the hexatic phase at

$\phi \approx 0.70$. This behaviour is very similar to results in [42] for experiments on NIPA particles and simulations of hard disks across the freezing transition, suggesting that the value of S_2 can be used to indicate the position of the freezing transition.

4. Conclusion

In summary, we have further elucidated the nature of melting in 2D hard spheres by studying three additional quantities known to show characteristic behaviour close to the liquid-hexatic and hexatic-crystal transitions. In particular, we first consider the bond-orientational correlation time as the hexatic phase is approached from the liquid. We find it shows evidence of a divergence associated with the onset of critical fluctuations, but that this is preempted by the weakly first order liquid-hexatic transition. We also compute Frank's constant, which in the hexatic phase is found to diverge upon approaching the crystal. Finally, we obtain the excess entropy from the calculation of the radial distribution functions for a wide range of area fractions across the liquid, hexatic and crystals phases and find that $-S_2/k_B$ appears to reach a characteristic value of 4.5 at the onset of the freezing transition in agreement with previous reports.

ORCID iDs

Roel P A Dullens ⬤ https://orcid.org/0000-0003-1751-0958

References

[1] Mermin N D and Wagner H 1966 Absence of ferromagnetism or antiferromagnetism in one-or two-dimensional isotropic Heisenberg models *Phys. Rev. Lett.* **17** 1133

[2] Wei Q H, Bechinger C and Leiderer P 2000 Single-file diffusion of colloids in one-dimensional channels *Science* **287** 625

[3] Di Leonardo R, Keen S, Ianni F, Leach J, Padgett M and Ruocco G 2008 Hydrodynamic interactions in two dimensions *Phys. Rev.* E **78** 031406

[4] Pusey P N and Van Megen W 1986 Phase behaviour of concentrated suspensions of nearly hard colloidal spheres *Nature* **320** 340

[5] Kosterlitz J M and Thouless D J 1973 Ordering, metastability and phase transitions in two-dimensional systems *J. Phys. C: Solid State Phys.* **6** 1181

[6] Halperin B I and Nelson D R 1978 Theory of two-dimensional melting *Phys. Rev. Lett.* **41** 121

[7] Nelson D R and Halperin B I 1979 Dislocation-mediated melting in two dimensions *Phys. Rev.* B **19** 2457

[8] Young A P 1979 Melting and the vector Coulomb gas in two dimensions *Phys. Rev.* B **19** 1855

[9] Zahn K, Lenke R and Maret G 1999 Two-stage melting of paramagnetic colloidal crystals in two dimensions *Phys. Rev. Lett.* **82** 2721

[10] Nelson D R 2002 *Defects and Geometry in Condensed Matter Physics* (Cambridge: Cambridge University Press)

[11] Keim P, Maret G and von Grünberg H H 2007 Frank's constant in the hexatic phase *Phys. Rev.* E **75** 031402

[12] Zahn K and Maret G 2000 Dynamic criteria for melting in two dimensions *Phys. Rev. Lett.* **85** 3656

[13] Han Y, Ha N Y, Alsayed A M and Yodh A G 2008 Melting of two-dimensional tunable-diameter colloidal crystals *Phys. Rev.* E **77** 041406

[14] Murray C A 1992 *Experimental Studies of Melting and Hexatic Order in Two-Dimensional Colloidal Suspensions* (New York: Springer) pp 137–215

[15] Alder B J and Wainwright T E 1962 Phase transition in elastic disks *Phys. Rev.* **127** 359

[16] Bladon P and Frenkel D 1995 Dislocation unbinding in dense two-dimensional crystals *Phys. Rev. Lett.* **74** 2519

[17] Bernard E P and Krauth W 2011 Two-step melting in two dimensions: first-order liquid-hexatic transition *Phys. Rev. Lett.* **107** 155704

[18] Kapfer S C and Krauth W 2015 Two-dimensional melting: from liquid-hexatic coexistence to continuous transitions *Phys. Rev. Lett.* **114** 035702

[19] Anderson J A, Antonaglia J, Millan J A, Engel M and Glotzer S C 2017 Shape and symmetry determine two-dimensional melting transitions of hard regular polygons *Phys. Rev.* X **7** 021001

[20] Deutschländer S, Horn T, Löwen H, Maret G and Keim P 2013 Two-dimensional melting under quenched disorder *Phys. Rev. Lett.* **111** 098301

[21] Qi W and Dijkstra M 2015 Destabilisation of the hexatic phase in systems of hard disks by quenched disorder due to pinning on a lattice *Soft Matter* **11** 2852

[22] Qi W, Gantapara A P and Dijkstra M 2014 Two-stage melting induced by dislocations and grain boundaries in monolayers of hard spheres *Soft Matter* **10** 5449

[23] von Grünberg H H, Keim P and Maret G 2007 Phase transitions in two-dimensional colloidal systems *Soft Matter* vol 3 (New York: Wiley) pp 40–83

[24] Gasser U, Eisenmann C, Maret G and Keim P 2010 Melting of crystals in two dimensions *ChemPhysChem* **11** 963–70

[25] Deutschländer S, Puertas A M, Maret G and Keim P 2014 Specific heat in two-dimensional melting *Phys. Rev. Lett.* **113** 127801

[26] Murray C A and Van Winkle D H 1987 Experimental observation of two-stage melting in a classical two-dimensional screened Coulomb system *Phys. Rev. Lett.* **58** 1200

[27] Marcus A H and Rice S A 1996 Observations of first-order liquid-to-hexatic and hexatic-to-solid phase transitions in a confined colloid suspension *Phys. Rev. Lett.* **77** 2577

[28] Karnchanaphanurach P, Lin B and Rice S A 2000 Melting transition in a quasi-two-dimensional colloid suspension: influence of the colloid–colloid interaction *Phys. Rev.* E **61** 4036

[29] Peng Y, Wang Z, Alsayed A M, Yodh A G and Han Y 2010 Melting of colloidal crystal films *Phys. Rev. Lett.* **104** 205703

[30] Lee J and Strandburg K J 1992 First-order melting transition of the hard-disk system *Phys. Rev.* B **46** 11190

[31] Zollweg J A and Chester G V 1992 Melting in two dimensions *Phys. Rev.* B **46** 11186

[32] Fernández J F, Alonso J J and Stankiewicz J 1995 One-stage continuous melting transition in two dimensions *Phys. Rev. Lett.* **75** 3477

[33] Jaster A 1999 Computer simulations of the two-dimensional melting transition using hard disks *Phys. Rev.* E **59** 2594

[34] Binder K, Sengupta S and Nielaba P 2002 The liquid-solid transition of hard discs: first-order transition or Kosterlitz–Thouless–Halperin–Nelson–Young scenario? *J. Phys.: Condens. Matter* **14** 2323

[35] Engel M, Anderson J A, Glotzer S C, Isobe M, Bernard E P and Krauth W 2013 Hard-disk equation of state: first-order liquid-hexatic transition in two dimensions with three simulation methods *Phys. Rev.* E **87** 042134

[36] Thorneywork A L, Abbott J L, Aarts D G A L and Dullens R P A 2017 Two-dimensional melting of colloidal hard spheres *Phys. Rev. Lett.* **118** 158001

[37] Thorneywork A L, Roth R, Aarts D G A L and Dullens R P A 2014 Communication: radial distribution functions in a two-dimensional binary colloidal hard sphere system *J. Chem. Phys.* **140** 161106

[38] Thorneywork A L, Rozas R E, Dullens R P A and Horbach J 2015 Effect of hydrodynamic interactions on self-diffusion of quasi-two-dimensional colloidal hard spheres *Phys. Rev. Lett.* **115** 268301

[39] Crocker J C and Grier D G 1996 Methods of digital video microscopy for colloidal studies *J. Colloid Interface Sci.* **179** 298

[40] Watanabe H, Yukawa S, Ozeki Y and Ito N 2004 Critical exponents of isotropic-hexatic phase transition in the hard-disk system *Phys. Rev.* E **69** 045103

[41] del Campo A 2015 Colloidal test bed for universal dynamics of phase transitions *Proc. Natl Acad. Sci. USA* **112** 6780

[42] Wang Z, Qi W, Peng Y, Alsayed A M, Chen Y, Tong Y and Han P 2011 Two features at the two-dimensional freezing transitions *J. Chem. Phys.* **134** 034506

[43] Baranyai A and Evans D J 1989 Direct entropy calculation from computer simulation of liquids *Phys. Rev.* A **40** 3817–22

[44] Ma X, Chen W, Wang Z, Peng Y, Han Y and Tong P 2013 Test of the universal scaling law of diffusion in colloidal monolayers *Phys. Rev. Lett.* **110** 078302